Journal of Applied Mechanics and Technical Physics, Vol. 41, No. 6, 2000

EFFECT OF EVAPORATION OF LIQUID DROPLETS ON THE DISTRIBUTION OF PARAMETERS IN A TWO-SPECIES LAMINAR FLOW

V. I. Terekhov, M. A. Pakhomov,[1] and V. V. Chichindaev[1]

UDC 536.24

A calculation model was developed, and the heat- and mass-transfer characteristics in a laminar air–vapor–droplet flow moving in a round tube were studied numerically. The distributions of parameters of the two-phase flow over the tube radius were obtained for varied initial concentrations of the gas phase. The calculated heat and mass transfer is compared to experimental data and calculations of other authors. It is shown that evaporation of droplets in a vapor–gas flow leads to a more intense heat release as compared to a one-species vapor–droplet flow and one-phase vapor flow.

Introduction. Theoretical research on problems of flow and heat-transfer simulation in two-phase and multispecies flows is described in [1–3].

The heat transfer in a two-phase gas–droplet flow containing small droplets of water may correspond to the presence or absence of a liquid film on the heated surface [1]. In the first case, which is observed for a comparatively low temperature of the wall, the boundary layer consists of two regions: an internal liquid layer on the wall and an external dispersed boundary layer. Aihara et al. [4] studied the heat transfer on a wedge-shaped body. An increase in heat transfer by a factor of 10 to 30 as compared to a one-phase gas flow was registered. The second case is characterized by the absence of the liquid film on the wall; it is observed under conditions where the liquid droplets evaporate before they reach the surface or at the moment of their deposition on the wall.

Heat transfer in a laminar mist flow on a dry isothermal plate was studied theoretically and experimentally in [5]. The effect of droplets and their evaporation on the boundary-layer structure was analyzed for the case of a low concentration of small particles of size up to 3 μm. A similar case of dispersed flow was studied taking into account heat transfer in various internal flow regimes [6–14]. As is shown in [6], apart from criteria that characterize the one-phase heat-transfer regime, there are three dimensionless parameters in a vapor–droplet flow, which determine the heat transfer in the two-phase flow regime. An analysis of their influence on heat-transfer intensity revealed the range of heat-transfer coefficients depending on the initial parameters, the length of the zone of existence of a two-phase flow, the character of droplet-diameter variation, and other features of heat transfer in a two-phase vapor–droplet flow. Crowe et al. [12] studied numerically the processes of momentum, energy, and mass transfer in a gas–droplet flow using the model droplet–internal drain [Particle-Source-In Cell (PSI-CELL)]. The model is based on a hypothesis according to which the droplets are an internal source of vapor mass, momentum, and energy in the gas phase. The PSI-CELL model takes into account complex processes between the phases typical of multiphase flows. This model is also applicable in studying combustion problems. Using this hypothesis, Sijercic′ et al. [13] constructed a model that takes into account the forces of drag and gravity.

Kutateladze Institute of Thermal Physics, Siberian Division, Russian Academy of Sciences, Novosibirsk 630090. [1]Novosibirsk State Technical University, Novosibirsk 630092. Translated from Prikladnaya Mekhanika i Tekhnicheskaya Fizika, Vol. 41, No. 6, pp. 68–77, November–December, 2000. Original article submitted January 28, 2000.

It should be noted that most numerical studies deal with heat and mass transfer in one-species vapor–droplet flows.

In this work, numerical schemes of the heat-transfer process are constructed, and a parametric analysis in laminar two-species gas–vapor–droplet flows is performed. The problem formulation as a whole is similar to those in [6, 7]. However, here we study more complex air–vapor–droplet flows, where it is necessary to solve jointly the energy and diffusion equations for the vapor–gas mixture. These studies are also of interest in practical applications for calculating systems of two-phase cooling of the elements of energy equipment, devices for air conditioning, and other devices of chemical technology and power engineering.

1. Formulation of the Problem. In this paper, we consider a two-dimensional stabilized steady two-phase gas–vapor–droplet flow in a tube, taking into account evaporation of liquid droplets. The present study was performed under conditions where the near-wall annular film of the liquid is already dry (i.e., the wall temperature is higher than the Leidenfrost temperature for droplets). Conductive heat transfer caused by the droplet–wall contact is negligibly small as compared to the contribution of convective heat transfer between the vapor and the wall [6]; radiant heat transfer is also ignored. The droplets in a vapor–gas flow serve as a distributed output of heat and a source of vapor. The mixture transfers heat to liquid droplets, and the vapor generated thereby is heated to the temperature of the main vapor–air flow.

It is known that the velocity profile of a one-phase liquid of a hydrodynamically stabilized surface has a parabolic form [15]. It was assumed that this shape of the profile is also retained for a two-phase flow, and droplet evaporation increases only the mass-mean velocity of the vapor as the dispersed mixture moves along the channel.

The temperature distribution of the vapor and droplets in the entrance cross section of the tube is uniform, and the vapor may be overheated above the saturation temperature at this partial pressure. The particle temperature over its diameter was also assumed to be constant, since according to the estimates of [16], the Biot number is $\mathrm{Bi} = \alpha_0 d_{P1}/\lambda_P < 0.1$, where α_0 is the heat-transfer coefficient of a nonevaporating particle, d_{P1} is the initial diameter of the droplet, and λ_P is the thermal conductivity of the liquid phase.

All particles at the tube entrance have an identical size, and the number of particles per unit volume (numerical concentration) is also constant, the latter condition being valid for the whole flow region. In zones where complete evaporation of droplets occurs, their numerical concentration is simulated by pseudoparticles of zero diameter.

The temperature gradient of the vapor–gas phase arising due to the heat transfer to the tube wall makes the evaporation process nonuniform over the tube radius; therefore, the particles in the near-wall region are smaller than those in the axial region. This, in turn, changes the mass concentrations of the gas, vapor, and liquid over the cross section and along the tube.

Two types of boundary conditions on the inner surface of the tube are considered: a regime with a constant heat-flux density on the wall ($q_W = \mathrm{const}$) and a regime with a constant temperature of the wall ($T_W = \mathrm{const}$). The case predominantly studied in this paper is $q_W = \mathrm{const}$.

2. Governing Equations and Boundary Conditions. At the section with a hydrodynamically stabilized flow, from the equation of motion for the streamwise velocity, we have a parabolic profile [15]:

$$W_X = 2\bar{W}[1 - (r/R_0)^2], \tag{1}$$

where $\bar{W}$ is the mean flow rate of the mixture in the current cross section of the tube, R_0 is the tube radius, and r is the current transverse coordinate.

Taking into account the assumptions used, we describe the heat and mass transfer in an axisymmetric vapor–gas–droplet flow by a system of energy and diffusion equations for a vapor–gas mixture [3, 7]:

$$2\rho_\Sigma C_{p\Sigma}\bar{W}\Big(1 - \Big(\frac{r}{R_0}\Big)^2\Big)\frac{\partial T}{\partial x}$$

$$= \frac{\lambda_\Sigma}{r}\frac{\partial}{\partial r}\Big(r\frac{\partial T}{\partial r}\Big) - \pi n d_P^2 \alpha_0 (T - T_P) + \rho_\Sigma D_{1-2}\frac{\partial K_V}{\partial r}(C_{pV} - C_{pA})\frac{\partial T}{\partial r}; \tag{2}$$

$$2\rho_\Sigma C_{p\Sigma}\bar{W}\Big(1-\Big(\frac{r}{R_0}\Big)^2\Big)\frac{\partial K_V}{\partial x}=\frac{\rho_\Sigma D_{1-2}}{r}\frac{\partial}{\partial r}\Big(r\,\frac{\partial K_V}{\partial r}\Big)+j_S\pi n d_P^2. \tag{3}$$

Here ρ_Σ and λ_Σ are the density and thermal conductivity of the vapor–air flow, α_0 is the coefficient of heat transfer to nonevaporating droplets, $C_{p\Sigma}$, C_{pA}, and C_{pV} are the specific heat capacity of the vapor–air mixture, air, and vapor, T and T_P are the temperatures of the mixture and the droplet, x is the longitudinal coordinate, n is the numerical concentration of liquid droplets in the tube, D_{1-2} is the coefficient of vapor-to-gas diffusion, K_V is the mass concentration of vapor in a binary vapor–air mixture, j_S is the transverse flow of vapor on the surface of the evaporating droplet, and d_P is the current diameter of the droplet.

The energy and diffusion equations have source (drain) terms that describe heat removal from the gas phase and vapor-mass supply due to evaporation of particles. They are represented by the second terms in the right part in Eqs. (2) and (3). In addition, the energy equation (2) in the right part contains a term caused by diffusive heat transfer in the vapor–gas phase.

Relations (2) and (3) are supplemented by the heat-transfer equation at the interface

$$C_{pP}\rho_P\,\frac{\pi d_P^3}{6}\,\frac{dT_P}{d\tau}=\alpha\pi d_P^2(T-T_P)-j_S\pi d_P^2[L+C_{pV}(T-T_P)] \tag{4}$$

(C_{pP} is the specific heat capacity of the liquid, ρ_P is the liquid density, α is the coefficient of heat removal of the evaporating droplet, and L is the latent heat of evaporation) and the equation of conservation of the vapor mass on the evaporating droplet surface [3]

$$j_S=j_S K_{VS}-\rho_V D_{1-2}\Big(\frac{\partial K_V}{\partial r}\Big)_S, \tag{5}$$

where K_{VS} is the mass concentration of vapor on the particle surface corresponding to saturation parameters at a droplet temperature of T_P. According to [17], the quantity α in (4) is related to the heat-transfer coefficient α_0 by the following formula:

$$\alpha=\frac{\alpha_0}{1+C_{p\Sigma}(T-T_P)/L}. \tag{6}$$

The heat-transfer law for a nonevaporating droplet is determined from Drake's formula [2]:

$$\mathrm{Nu}=2+0.457\,\mathrm{Re}_P^{0.55}\,\mathrm{Pr}^{1/3}, \tag{7}$$

where Nu is the Nusselt number, $\mathrm{Re}_P=\Delta W d_P/\nu_\Sigma$ is the particle Reynolds number based on the phase-slip velocity, ΔW is the velocity of the vapor–air mixture relative to the droplet, ν_Σ is the viscosity of the vapor–air mixture, and Pr is the Prandtl number of the mixture. The heat-transfer coefficient to finely dispersed droplets in the absence of phase slipping is described by the relation $\mathrm{Nu}=\alpha_0 d_P/\lambda_\Sigma=2$; hence, we have $\alpha_0=2\lambda_\Sigma/d_P$.

Taking into account that the diffusion Stanton number is determined as

$$\mathrm{St}_D=-\rho_V D_{1-2}\Big(\frac{\partial K_V}{\partial r}\Big)_S\Big/\rho_\Sigma\Delta W(K_{VS}-K_V), \tag{8}$$

the equation of conservation of mass (5), taking into account Eq. (8), can be written in the form

$$j_S=\mathrm{St}_D\rho_\Sigma\Delta W b_{1D}, \tag{9}$$

where

$$b_{1D}=(K_{VS}-K_V)/(1-K_{VS}) \tag{10}$$

is a diffusion parameter of vapor blowing from the evaporating particle and ρ_V is the vapor density.

For finely dispersed particles in the absence of phase slipping ($\Delta W=0$), the mass transfer between the droplets and the mixture is described by the known relations [3] $\mathrm{Sh}=\beta d_P/D_{1-2}=2$ and $\mathrm{St}_D=(\mathrm{Sh}/\mathrm{Re}_P)\,\mathrm{Sc}=(2/\mathrm{Re}_P)\,\mathrm{Sc}$, where Sh and Sc are the Sherwood and Schmidt numbers, respectively, and β is the mass-transfer coefficient. Then Eq. (9) is transformed to

$$j_S=2D_{1-2}\rho_V b_{1D}/d_P, \tag{11}$$

and the permeability parameter b_{1D} is determined from Eq. (10) using the saturation curve.

The equation of material balance for a binary vapor–air mixture has the form

$$K_V + K_A = 1, \tag{12}$$

where K_A is the mass concentration of air in the binary vapor–air mixture. For a ternary mixture vapor–gas–liquid, this equation is written as

$$C_V + C_A + C_L = 1, \tag{13}$$

where C_V, C_A, and C_L are the mass concentrations of the vapor, air, and liquid.

The relations between the values of mass concentrations may be written in the following form:

$$K_V = \frac{C_V}{C_V + C_A}, \qquad K_A = \frac{C_A}{C_V + C_A} = 1 - K_V. \tag{14}$$

The expression for calculating the current diameter of the droplet d_P is obtained from the relation

$$C_P = m_P n, \tag{15}$$

where m_P is the mass of the liquid particle. After transformations, taking into account that $m_P = \rho_P \pi d_P^3 n/6$, we obtain from (15)

$$d_P = \sqrt[3]{\frac{6C_P}{\pi \rho_P n}}. \tag{16}$$

Relations (2)–(16) form a closed system of equations that describe the heat- and mass-transfer processes in a vapor–gas–droplet flow and allow one to calculate all the sought quantities (temperature distribution, enthalpy, and concentrations of the phases and components of the vapor–gas mixture), determine the character of variation of particle sizes, and analyze the degree of heat-transfer intensification due to the evaporation processes.

The boundary conditions for the temperature and concentration of the components of the vapor–gas mixture are written in the form

$$\frac{\partial T}{\partial r} = 0, \quad \frac{\partial K_V}{\partial r} = 0, \quad \frac{\partial U}{\partial r} = 0 \quad \text{for} \quad r = 0,$$

$$\lambda_\Sigma \frac{\partial T}{\partial r} = q_W \quad (q_W = \text{const}) \quad \text{or} \quad T = T_W = \text{const}, \quad \frac{\partial K_V}{\partial r} = 0 \quad \text{for} \quad r = R_0.$$

The temperature of the vapor–gas mixture and particles at the entrance and the concentrations of the vapor, gas, and droplets were assumed to be constant over the cross section: $T = T_1$, $T_P = T_{P1}$, $d_P = d_{P1}$, $K_V = K_{V1}$, $K_A = 1 - K_{V1}$, and $C_P = C_{P1}$ for $x = 0$.

The Nusselt number for a constant heat-flux density on the wall was determined from the difference between the wall temperature and the mass-mean temperature of the vapor–gas mixture:

$$\text{Nu} = \frac{q_W 2R_0}{\lambda_\Sigma (T_W - T_m)}. \tag{17}$$

The mass-mean temperature in (17) was found by integration of the temperature field over the tube cross section:

$$T_m = \frac{4}{R_0^2} \int_0^{R_0} T\Big(1 - \Big(\frac{r}{R_0}\Big)^2\Big) r\, dr.$$

The concentrations of components of the gas and liquid phases averaged over the tube diameter were calculated in a similar manner.

3. Calculation Algorithm and Verification of Reliability of the Numerical Model. Equations with the corresponding boundary conditions were solved numerically using finite-difference schemes. The algebraic system was solved using the Thomas algorithm [18]. The steps in the longitudinal and transverse directions were 1 and 0.01 diameter, respectively. The tube length was 2 m and its inner diameter was 0.02 m. The thermophysical properties were calculated using the formulas derived in [19].

In the absence of the liquid phase and air, the numerical solution with an error of less than 2% corresponds to the numerical solution of the problem of heat transfer in a stabilized one-phase flow, which was proposed by Kutateladze [15]. For comparison, the data of the numerical analysis of [6] were used in the two-phase flow regime. Good agreement was obtained between the calculations by the present model and numerical calculations for a stabilized vapor–droplet flow [7].

4. Calculation Results, Discussion, and Comparison with Experiment. The results of studying the effect of parameters of a two-phase flow on heat and mass transfer in the tube are presented below. The main focus was on the effect of the gas concentration on the change in flow characteristics and heat-transfer intensification. The data obtained in the present work were compared to the results of [7] on heat transfer in vapor–droplet flows for a gas concentration of $C_A = 0$.

The calculations were performed for a mixture of water vapor and air (at atmospheric pressure) in the presence of liquid particles of water in the mixture. The initial parameters were varied within the following ranges: the temperature of the vapor–gas mixture at the entrance was 100–150°C, the flow velocity was 0–2 m/sec, the flow Reynolds number was 200–2000, the droplet diameter was 1–100 μm, and the mass concentrations of droplets and air were 0–0.1 and 0–0.8, respectively. The calculations yielded the temperatures of droplets and the vapor–air mixture, the mass concentrations of all components, the droplet diameter, and the heat transfer to the tube surface.

Figure 1 shows the calculation results in the form of dimensionless temperature profiles $\Theta = (T - T_W)/(T_0 - T_W)$ over the tube cross section for various values of the mass concentration of air. The fixed quantity in these calculations was the Reynolds number based on the input parameters. Curve 1 in Fig. 1 is the temperature profile in the one-phase vapor–flow regime, and curve 2 refers to the vapor–droplet flow without air ($C_{A1} = 0$). As is shown in Fig. 1, an increase in the concentration of air at the entrance increases the fullness of the temperature profile, which intensifies the process of heat transfer to the tube surface. The calculations show that this pattern is observed for different flow rates and phase concentrations at the tube entrance.

The greater fullness of the temperature profile is primarily caused by the more active heat exchange between the droplets and vapor–gas mixture with a high concentration of air during evaporation. Indeed, with increasing C_{A1}, the diffusive transfer of vapor from the particle surface to the ambient flow increases, which increases the droplet-evaporation rate.

Figure 2 shows the calculation results for the particle size for different concentrations of air, other conditions being equal. An analysis of the data in Fig. 2 allows us to draw the following conclusions. The evaporation processes are more intense in the near-wall zone with a higher temperature. The small plateau near the tube centerline, especially for low concentrations of air, is caused by the low value of the temperature gradient in this region and, as is shown below, by the higher relative mass concentration of vapor in the axial region. The main conclusion is the significant decrease in the droplet size with increasing concentration of air in the mixture. The zone of the one-phase flow regime, where liquid droplets are absent, significantly increases (Fig. 2).

Obviously, the processes of heat and mass exchange between the liquid phase and the vapor–gas mixture and also the heat exchange with the tube surface are interrelated. Therefore, a more detailed description of the mechanism of heat- and mass-transfer processes requires the study of evolution of the concentration profiles of both the liquid phase and the components of the vapor–gas mixture along the tube (Fig. 3). The mass concentration of the liquid phase (Fig. 3a) decreases continuously along the channel, and the concentration of the vapor being formed (Fig. 3b) increases; in particular, for the conditions considered ($C_{P1} = C_{V1} = 0.1$)

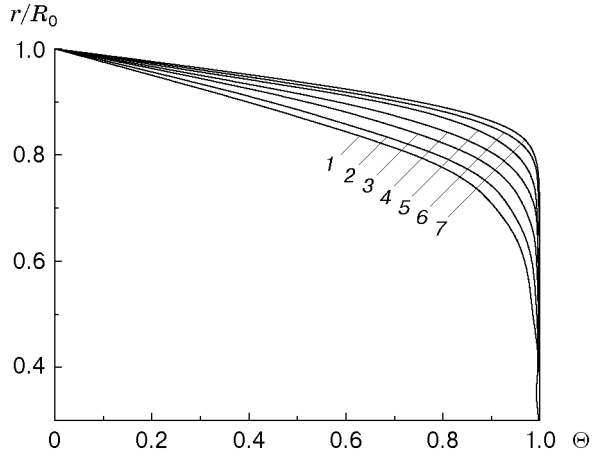

Fig. 1

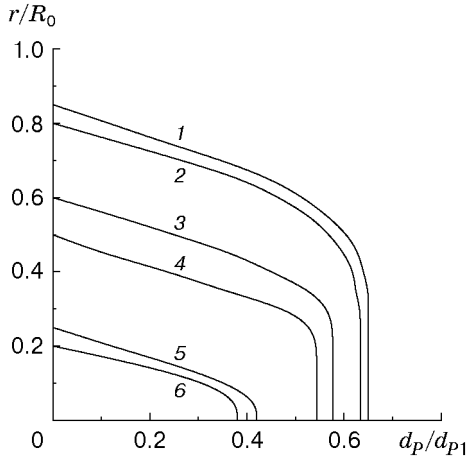

Fig. 2

Fig. 1. Distribution of the temperature profile of the air–vapor–droplet mixture over the tube radius for different mass concentrations of air at the entrance ($x/D = 5$, $d_{P1} = 30$ μm, $\mathrm{Re}_D = 1800$, $q_W = 200$ W/m^2, $T_1 = 373$ K, $T_{P1} = 283$ K, and $C_{P1} = 0.1$) for $C_{A1} = C_{P1} = 0$ (1) and $C_{A1} = 0$ (2), 0.01 (3), 0.1 (4), 0.2 (5), 0.5 (6), and 0.8 (7).

Fig. 2. Size of evaporating droplets versus the mass concentration of air (parameters are the same as in Fig. 1) for $C_{A1} = 0$ (1), 0.01 (2), 0.1 (3), 0.2 (4), 0.5 (5), and 0.8 (6).

as $x/D \to 10$, it increases twofold. The mass concentration of air is distributed nonmonotonically over the tube radius (Fig. 3c). Local minima of the concentration of air are formed in regions of the most intense evaporation; moving along the tube, these minima become less pronounced and are shifted toward the tube centerline.

The parameter of heat-transfer intensification, which is the ratio $\mathrm{Nu}/\mathrm{Nu}_0$, where Nu_0 is the Nusselt number in the one-phase vapor flow for an identical Reynolds number at the entrance, depends on the above-mentioned features of the structure of thermal fields and concentrations of the two-phase vapor–gas–droplet flow. The results of these calculations are plotted in Fig. 4. The heat-transfer intensification is the least ($\mathrm{Nu}/\mathrm{Nu}_0 < 1.5$) for the one-species vapor–droplet flow (curve 1). As the mass concentration of air increases, the heat transfer becomes noticeably more intense, but the length of the zone of intensified heat transfer along the channel significantly decreases.

The data in Fig. 4 should be considered as an illustration, since the process considered is multiparametric; hence, the degree of intensification is a function of a large number of thermodynamic parameters. A detailed study of their effect on the heat-transfer processes is outside the scope of the present work.

The hypotheses on which the model proposed was based were verified by an indirect comparison with available experimental data on heat transfer.

There are a limited number of papers that contain data on heat transfer in two-phase vapor–gas–droplet flows in tubes. Hishida et al. [10] considered a developing laminar mist flow at the initial section of a plane channel; therefore, the results obtained in that work cannot be used for comparison with the numerical model developed. There are almost no experimental data in the literature for a hydrodynamically stabilized vapor–gas–droplet flow in a tube. An exception is [8], where the process of heat transfer in the flow of a water–air aerosol in a compact heat exchanger was studied. The results of [8] were used for comparison with the present calculations (the change in the wall temperature along the heat-exchange section was compared). The calculations and experiments were performed for the following test-section parameters: length $l = 0.24$ m, equivalent diameter of the tube $d_{\mathrm{eq}} = 2.67$ mm, $x/D = 0$–80, maximum Reynolds number $\mathrm{Re}_{\mathrm{eq}} = 8 \cdot 10^3$, mass concentration of droplets $C_{P1} = 0$–0.03, and droplet diameter $d_{P1} = 1$–2 μm. The experiments were performed in the regime of a constant heat flux on the wall ($q_W = \mathrm{const}$).

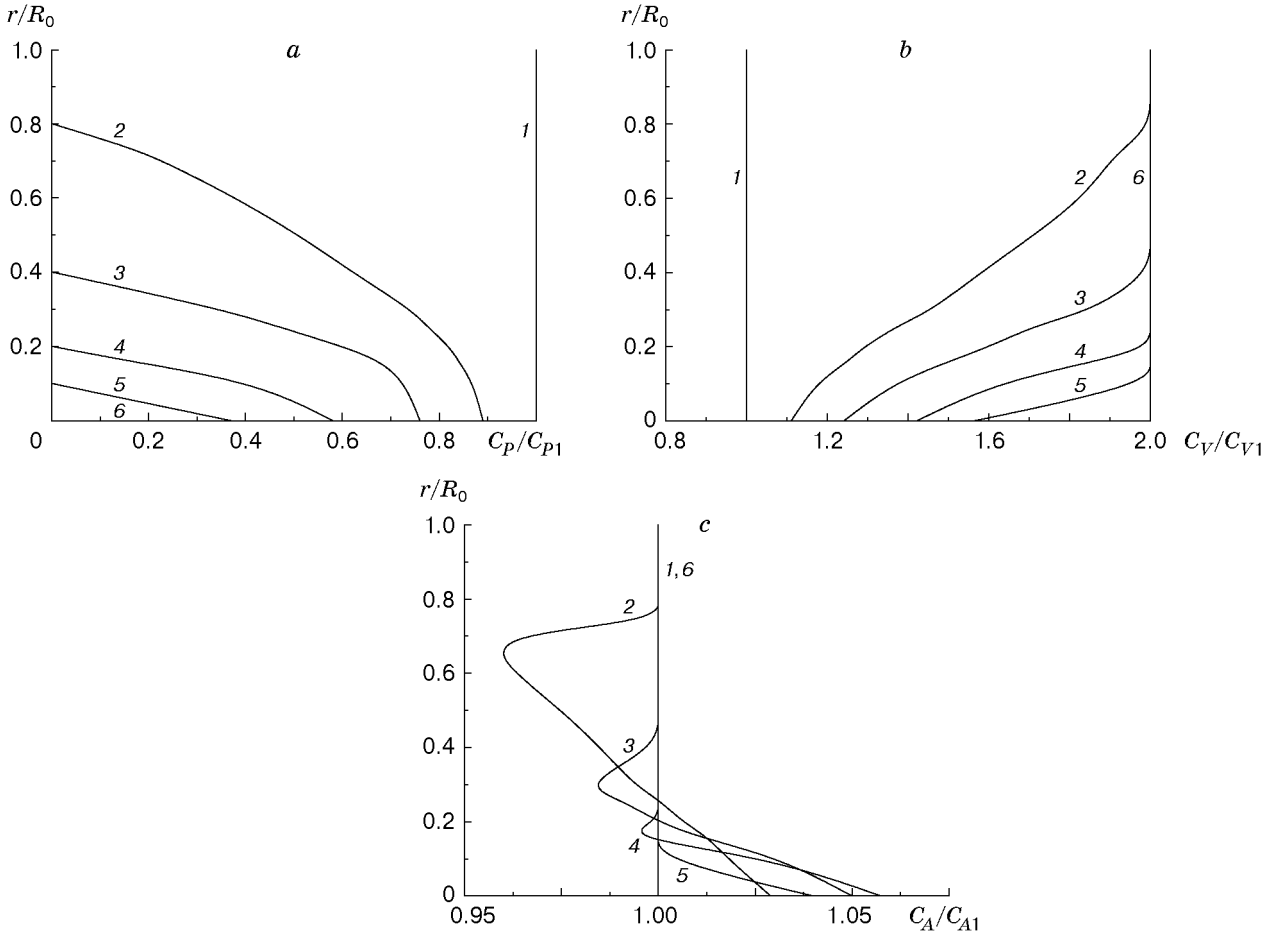

Fig. 3. Distribution of the mass concentration of the components of the mixture over the tube radius for the liquid phase (a), vapor (b), and air (c) (parameters are the same as in Fig. 1) for $x/D = 0$ (1), 1 (2), 2 (3), 5 (4), 7 (5), and 10 (6).

The numerical and experimental data are compared in Fig. 5, which shows the wall-temperature distribution along the tube of the heat-exchange channel. It follows from Fig. 5 that the calculation results by the present model are in good agreement with the experimental data. A typical behavior of the wall temperature for the calculated and experimental data is its monotonic increase along the channel. The more significant discrepancy between the calculated and experimental data in the beginning of the channel is explained by the influence of the initial section, which is associated with the development of a dynamic boundary layer in the experiments. The difference between the calculated and experimental data in this region is 20–25%. The difference on the major part of the channel is less than 10%.

Thus, the model developed gives an adequate qualitative and quantitative description of the heat and mass transfer in a two-species, two-phase flow in the presence of phase transformations. At the same time, this model cannot describe all the special features of interrelated dynamic and heat- and mass-transfer processes. The construction of such a model requires more detailed experimental and numerical studies.

Conclusions. A physical model of the joint heat and mass transfer in a laminar gas–vapor–droplet flow in a tube was developed. In this model, the liquid phase is a localized output of heat and a source of mass (vapor). A closed system of transport equations is derived, which includes the equation of energy with a source term, the diffusion equation for the vapor–gas mixture with a source, and the equations of heat and mass transfer for a single droplet. A numerical algorithm for solving this system of equations was developed.

The heat and mass transfer in a laminar two-phase vapor–droplet flow in a round tube was numerically studied.

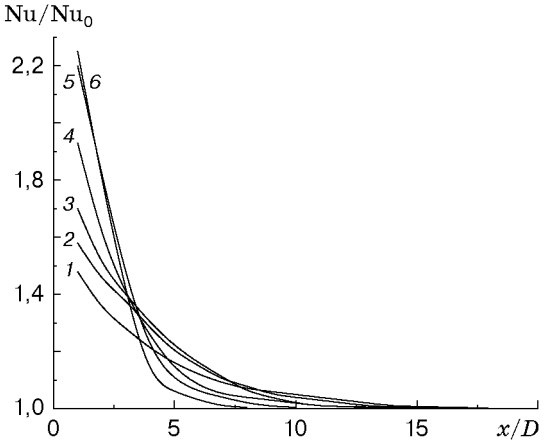

Fig. 4

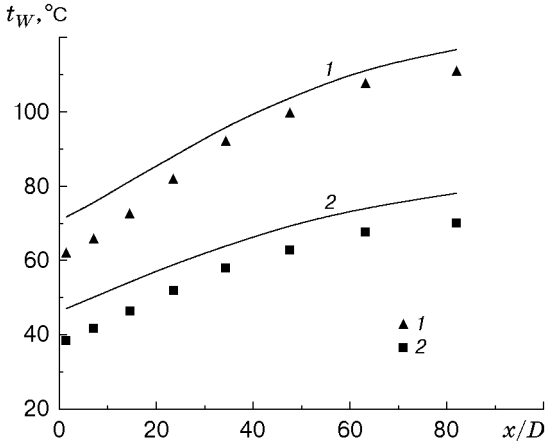

Fig. 5

Fig. 4. Distribution of the heat-transfer intensification parameter in the vapor–gas–droplet flow along the tube (parameters the same as in Fig. 1) for $C_{A1} = 0$ (1), 0.01 (2), 0.1 (3), 0.2 (4), 0.5 (5), and 0.8 (6).

Fig. 5. Wall-temperature distribution along the tube for $q_W = 0.8$ (1) and 0.4 kW/m^2 (2); the curves and points refer to the calculation and experiment [8], respectively.

It is shown that an increase in the mass concentration of air leads to the intensification of heat transfer as compared to a one-species flow. A comparison of the calculated results with experimental data demonstrates their qualitative and quantitative agreement.

This work was performed within the framework of the Federal goal-oriented program "State support of integration of higher education and fundamental science" (grant No. 330) and was supported by the Russian Foundation for Fundamental Research (grant No. 98-02-17898).

REFERENCES

1. R. I. Nigmatulin, *Dynamics of Multiphase Media*, Hemisphere, New York (1991).
2. S. L. Soo, *Fluid Dynamics of Multiphase Systems*, Blaisdell, Waltham (1967).
3. S. I. Isaev, I. A. Kozhinov, V. I. Kofanov, et al., *Theory of Heat and Mass Transfer* [in Russian], Izd. Mosk. Tekh. Univ., Moscow (1997).
4. T. Aihara, M. Taga, and T. Haraguchi, "Heat transfer from a uniform heat flux wedge in air-water mist flow," *Int. J. Heat Mass Transfer*, **22**, No. 1, 51–60 (1979).
5. J. W. Heyt and P. S. Larsen, "Heat transfer to binary mist flow," *Int. J. Heat Mass Transfer*, **14**, No. 9, 1395–1405 (1971).
6. Shi-chune Yao and A. Rane, "Heat transfer of laminar mist flow in tubes," *Teploperedacha*, **102**, No. 4, 93–101 (1980). (Transl. *Trans. ASME, J. Heat Transfer.*)
7. V. I. Terekhov, M. A. Pakhomov, and A. V. Chichindaev, "Heat transfer in a developed laminar vapor–droplet flow in a tube," *Teplofiz. Aéromekh.* (in press).
8. A. V. Chichindaev, "Heat transfer to a low-temperature flow of water aerosol," Candidate's Dissertation in Tech. Sci., Novosibirsk (1998).
9. E. N. Ganic′ and W. M. Rohsenow, "Dispersed flow heat transfer," *Int. J. Heat Mass Transfer*, **20**, No. 8, 855–865 (1977).
10. K. Hishida, M. Maeda, and S. Ikai, "Heat transfer from a plate in two-component mist flow," *Teploperedacha*, **102**, No. 3, 143–150 (1980). (Transl. *Trans. ASME, J. Heat Transfer.*)
11. V. T. Buglaev and A. S. Strebkov, "Simulation results for heat transfer in the case of evaporating cooling of a gas flow by droplet moisture," in: *Proc. II Ross. National Conf. on Heat Transfer* (Oct. 20–23, 1998) [in Russian], Vol. 4, Izd. Mosk. Énerg. Inst., Moscow (1998), pp. 268–272.

12. C. T. Crowe, M. P. Sharma, and D. E. Stock, "The Particle-Source-In Cell (PSI-CELL) model for gas–droplet flows," *Trans. ASME, J. Basic Eng.*, **99**, No. 2 (1977).
13. M. Sijercic′, G. Zivkovic′, and S. Oka, "The comparison of stochastic and diffusion models of dispersed phase in two-phase turbulent flow," in: *Proc. of the 1st Int. Symp. on Two-Phase Modeling and Experiment* (Rome, Italy, May 5–9, 1995), Vol. 1, Edizioni ETS, Pisa (1995), pp. 375–382.
14. A. Berlemont, M.-S. Grancher, and G. Gousbet, "On the lagrangian simulation of turbulence on droplet evaporating," *Int. J. Heat Mass Transfer*, **34**, No. 9, 2805–2812 (1991).
15. S. S. Kutateladze, *Fundamentals of Heat-Transfer Theory* [in Russian], Atomizdat, Moscow (1979).
16. A. V. Lykov, *Theory of Thermal Conductivity* [in Russian], Vysshaya Shkola, Moscow (1967).
17. M. C. Yuen and L. W. Chen, "Heat transfer measurements of evaporating liquid droplets," *Int. J. Heat Mass Transfer*, **21**, No. 2, 537–542 (1978).
18. T. Shih, *Numerical Heat Transfer*, Hemisphere Publ. Co., Washington (1984).
19. T. Fujii, *Theory of Laminar Film Condensation*, Springer-Verlag, New York (1991).